ISBN: 978-3-95450-184-7 doi:10.18429/JACoW-IPAC2018-TUPML059

SLICE ENERGY SPREAD OPTIMIZATION FOR A 5 GeV LASER-PLASMA ACCELERATOR

X. Li*, P. A. P. Nghiem, A. Mosnier, CEA/IRFU, Gif-sur-Yvette, France

Abstract

GeV-scale laser-plasma accelerating modules can be integrated into a multi-staged plasma linac for driving compact X-ray light sources or future colliders. Such a plasma module, operating in the quasi-linear regime, has been designed for the 5 GeV laser plasma acceleration stage (LPAS) of the EuPRAXIA project. Although it can be employed to optimize the total energy spread, the beam loading effect introduces an non-negligible slice energy spread to the beam. In this paper, we study the slice energy spread from linear theory, establishing a relationship between it and the laser-plasma parameters. To reduce the slice energy spread, simulations have been carried out for various plasma densities and laser strengths. The results will be discussed and compared with the theory.

INTRODUCTION

Plasma-based accelerators [1, 2] have been considered as promising candidates to drive compact X-ray light sources [3] or future lepton colliders [4] because of their ability to provide extremely high accelerating fields. Being free of the breakdown as in conventional RF structures, an ionized plasma could sustain a plasma wave with electric fields in excess of the cold nonrelativistic wave breaking field, $E_0 = m_e c\omega_p/e$ or $E_0(\mathrm{V/m}) \simeq 96\sqrt{n_p(\mathrm{cm}^{-3})}$, where ω_p is the plasma wave frequency, m_e and e are electron rest mass and charge, respectively, c is the speed of light in vacuum and n_p is the plasma density. Due to the difficulty of laser guiding and the depletion of laser power in a long plasma, a plasma module could just accelerate the electrons to multi-GeV scale. To achieve a final beam energy of a few hundreds of GeV or even TeV, it is necessary to construct a multi-staged plasma linac. For successful staging, the beam quality out of one module is important.

In this paper, we investigate the plasma module from the aspect of the slice energy spread in the context of the EuPRAXIA project, where a 30 pC electron beam of ~150 MeV (externally injected from a plasma or RF injector) is accelerated to 5 GeV in a laser-plasma acceleration stage (LPAS) [5, 6]. To allow better stability, the plasma wave is operated in the linear or quasi-linear regime, which requires a laser strength of $a_0 \geq 1$. While it is used to minimize the total energy spread, the beam loading effect also causes a non-negligible slice energy spread due to its strong radial dependence across the beam. Here we report the theoretical analysis of the slice energy spread, starting from linear theory, to establish a relationship between the slice energy spread and the laser-plasma parameters. Based on it, 3D simulations by the Warp [7] codes have carried out for various laser-plasma parameters and the results will be discussed and compared with the theory.

THEORIES

The Beam Loading Effect

In LPAS, the witness beam can excite a co-moving plasma wave when it moves through the plasma. The process that the wave produced by the accelerated beam modifies the fields in the plasma is referred to as beam loading. In the linear or quasi-linear regime, the beam loading effect can be calculated using perturbation theory. For an arbitrary relativistic electron density of the form $n_b(\xi, r) = n_{||}(\xi)n_\perp(r)$, where $\xi = z - ct$, the longitudinal component can be written into [8]

$$E_z^b(\xi, r) = \frac{e}{\epsilon_0}\int_{-\infty}^{\xi} n_{||}(\xi')\cos[k_p(\xi - \xi')]d\xi' \cdot R(r), \quad (1)$$

$$R(r) = k_p^2 \int_0^\infty r'\mathrm{d}r' n_\perp(r')K_0(k_p|\vec{r} - \vec{r}'|). \quad (2)$$

where $k_p = \omega_p/c$ is the plasma wavenumber, ϵ_0 is the electric constant, K_0 is the zeroth-order modified Bessel function. Since it's very difficult to get an analytical expression for E_z^b, we try to find an approximate one for a bi-gaussian bunch profile, that is, $n_b(\xi, r) = n_b \exp\left(-\xi^2/2\sigma_z^2\right)\exp\left(-r^2/2\sigma_r^2\right)$, with $en_b = Q_b/(2\pi)^{1.5}\sigma_z\sigma_r^2$, σ_r the rms beam size and σ_z the rms bunch length, Q_b the bunch charge. For this specific profile, the on-axis longitudinal field, to the first order, is

$$E_z^b(\xi) \simeq E_z^b(0) + E_z'(0)\xi = E_z^b(0)\left[1 + \frac{E_z'(0)}{E_z^b(0)}\xi\right], \quad (3)$$

with

$$E_z^b(0) = \frac{Q_b}{4\pi\epsilon_0}k_p^2 e^{-\frac{k_p^2\sigma_z^2}{2}}\left[0.058 - \ln(k_p\sigma_r)\right]$$
$$\propto Q_b n_p\left[0.058 - \ln(k_p\sigma_r)\right] \quad (4)$$

$$E_z'(0)/E_z^b(0) = \sqrt{\frac{2}{\pi}}\sigma_z^{-1}\left(1 - \frac{k_p^2\sigma_z^2}{2}\right), \quad (5)$$

where $E_z^b(0)$ and $E_z'(0)$ are the electric field and its derivative at $\xi = 0, r = 0$, respectively. The limits $k_p\sigma_r \ll 1$ and $k_p\sigma_z \ll 1$ have been used to derive the equations.

In Fig. 1(a), the on-axis longitudinal field estimated by Eq. (4) was compared with that calculated by Eq. (1). They agreed very well between $-\sigma_z < \xi < \sigma_z$, in which most of the electrons reside. The longitudinal field was also plotted as a function of transverse coordinate for various beam size in Fig. 1(b), showing a strong transverse dependence.

* xiangkun.li@cea.fr

ISBN: 978-3-95450-184-7 doi:10.18429/JACoW-IPAC2018-TUPML059

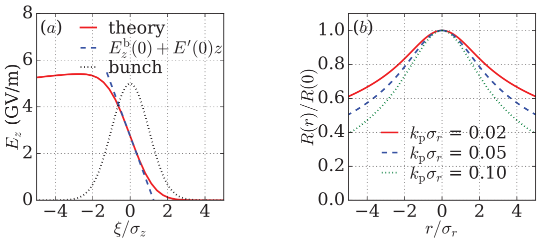

Figure 1: (a) Longitudinal and (b) radial distributions of E_z^b.

The Slice Energy Spread

Assume that the accelerating field experienced by one particle is the sum of the laser-driven wakefield and the beam-driven wakefield or beam loading effect, that is

$$E_{\text{acc}}(\xi, r, z) = E_z^{\text{LW}}\left(r, z+\xi\right) + E_z^{\text{b}}(\xi, r, z), \tag{6}$$

where z is the longitudinal coordinate of the reference particle in the laboratory frame, ξ is the longitudinal coordinate within the bunch. The laser-driven wakefield has the form of $E_z^{\text{LW}}(r) \sim \exp(-2r^2/w_0^2)$ and is r-independent near the axis when the laser spot size is much larger than the beam size [2]. However, the beam loading effect, which can be written as $E_z^{\text{b}}(\xi, r, z) = E_z^{\text{b}}(\xi, z)\hat{R}(r)$, with $\hat{R}(r) = R(r)/R(0)$, has a significant radial dependence.

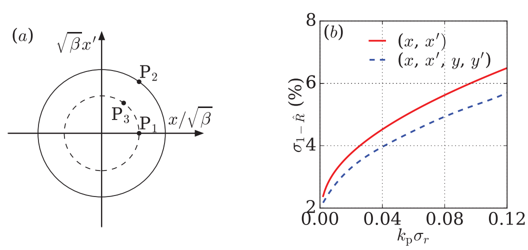

Figure 2: (a) Illustration of particle's motion in 2D normalized trace space and (b) dependence of slice energy spread on the normalized beam size in 2D and 4D trace space.

The radial coordinate of one particle is difined by the betatron motion and therefore is a function of time,

$$r^2 = A_x^2 \cos^2\phi_x + A_y^2 \cos^2\phi_y, \tag{7}$$

where A_x and A_y are oscillation amplitudes, which follows the same distribution as $n_\perp$, ϕ_x and ϕ_y are time-dependent phases in $x - x'$ and $y - y'$ phase spaces, respectively. Since they have the same betatron frequency, it takes the same time for all the particles to undergo one turn of betatron oscillation. And it is reasonable to compare their energy gain only after they have all gone through one or multiple turns of oscillation. To illustrate this, consider the motion of particles in the normalized trace space $(x/\sqrt{\beta}, \sqrt{\beta}x')$, with β the betatron amplitude. In LPAS, the oscillation is much faster than the change of the force and the beam energy because of the strong focusing force. Therefore, we could assume a constant betatron amplitude during one turn. As shown in Fig. 2(a), the energy gains of P_1 and P_2 will be different after one turn, because they have different trajectories in the trace space, which means different transverse coordinates. On the contrary, P_1 and P_3 will gain the same energy after one turn, because they have the same trajectories in the trace space, which means the same transverse coordinates.

To estimate the slice energy spread, we made the following assumptions. First, we neglect the change in the beam energy during one betatron oscillation period as mentioned above. Secondly, we assume that the beam size doesn't change significantly during the acceleration, which almost holds when the beam energy goes very high. Thirdly, we also assume that the plasma density the beam sees is the same despite the dephasing effect. With the last two assumptions, the beam loading effect is unchanged throughout the acceleration, or $E_z^{\text{b}}(\xi, z) = E_z^{\text{b}}(\xi)$.

For a slice located at ξ, the energy gain deviation between an off-axis particle and an on-axis particle is $eE_z^{\text{b}}(\xi)\left[1 - \hat{R}(r)\right]\text{d}z$. The radial dependence term $1 - \hat{R}(r)$ is a function of the oscillation amplitudes and phases through Eq. (7), and is averaged for one period of betatron motion (e.g., $-\pi < \theta_x < \pi$). Using a Monte-Carlo method, we obtained the root mean square of this term, which turned out to be a function of the normalized beam size $k_\text{p}\sigma_r$, as shown in Fig. 2(b). The rms slice energy spread then is

$$\sigma_{E_s} = \int_0^{L_{\text{acc}}} eE_z^{\text{b}}(\xi)\text{d}z \cdot \sigma_{1-\hat{R}} = eE_z^{\text{b}}(\xi)L_{\text{acc}} \cdot \sigma_{1-\hat{R}}, \tag{8}$$

where L_{acc} is the accelerating length. And, the relative slice energy spread is

$$\sigma_{E_s}/E = \frac{eE_z^{\text{b}}(\xi)L_{\text{acc}} \cdot f_\perp}{W_b} \simeq \frac{E_z^{\text{b}}(\xi)}{\langle E_{\text{acc}}\rangle} \cdot \sigma_{1-\hat{R}}, \tag{9}$$

where W_b is the final beam energy and $\langle E_{\text{acc}}\rangle \simeq \Delta W_\text{b}/L_{\text{acc}}$ is the average accelerating field.

SIMULATIONS AND DISCUSSIONS

The main parameters used in the simulations are listed in Table 1. To minimize the slice energy spread, we have carried out simulations with different laser and plasma parameters. For each set of parameters, the plasma channel, the beam size and the bunch length have been optimized first [6]: a good channel depth is chosen so that the laser propagates without neither significant over-focusing nor de-focusing; the beam size is matched to the transverse focusing force at the entrance and the bunch length is scanned to minimize the total energy spread.

According to Eq. (9), the slice energy spread could be reduced in several ways, such as tuning the plasma density. In so doing, both E_z^{b} and $\langle E_{\text{acc}}\rangle$ will change, but in a different way. That's because the accelerating field does not only depend on the plasma density but also on the dephaing effect. In our simulations, three plasma densities were compared while keeping the laser strength of $a_0 = \sqrt{2}$. The slice energy spread at the bunch center was shown as a function

ISBN: 978-3-95450-184-7 doi:10.18429/JACoW-IPAC2018-TUPML059

Table 1: Simulation Parameters for the LPAS

variable	value	unit
Laser		
strength a_0	1 – 2	
spot size $k_p w_0$	~ 3	
duration $k_p \sigma_L$	$\sqrt{2}$	
Plasma		
density n_p	1 – 2	10^{17} cm^{-3}
acc. length L_{acc}	~ 30	cm
channel depth $\Delta n/\Delta n_c$	< 1	
Electron		
charge Q	30	pC
energy E_k	150	MeV
energy spread $\Delta E/E$	0.5	%
beam size σ_x	~1	μ m
emittance $\varepsilon_{n,x}$	1.0	π mmmrad
bunch length σ_z	1 – 3	μm

of the plasma density in Fig. 3(a). For the theoretical estimation from Eq. (9), the plasma density and beam size at 5 GeV were considered. The deviation, especially at lower plasma density, was probably due to the fact that the linear theory doesn't work well when the beam density is much higher than the plasma density [9]. For the plasma density of 1.0× 10^{17} cm^{-3}, simulation was also carried out with a higher laser strength ($a_0 = 2$). The increased accelerating field helped reduce the slice energy spread further to be below 0.1%, as required by the X-ray FEL [5].

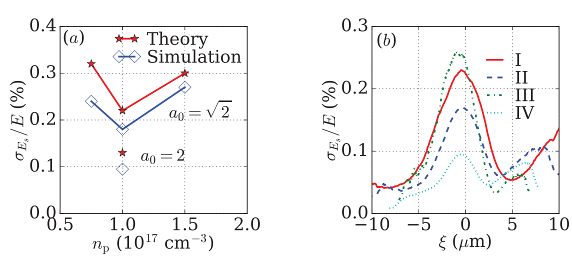

Figure 3: (a) Slice energy spread at the bunch center ($\xi = 0$) as a function of the plasma density and laser strength; (b) slice energy spread distributions for $a_0 = \sqrt{2}$ and $n_p = 0.5, 1.0, 1.5 \times 10^{17}$cm^{-3} (I to III) and for $a_0 = 2$ and $n_p = 1.0 \times 10^{17}$cm^{-3} (IV).

The slice energy spread distributions are shown in Fig. 3(b). It's worth noting that for all the cases, the slice energy spread peaked near the bunch center, while according to Fig. 1(a) and Eq. (9), it would be higher near the bunch tail, where E_z^b is larger. This can be explained by Fig. 4, where a uniform transverse distribution around the axis was observed near the bunch tail. Due to the much higher beam density, plasma electrons are expelled by the space charge field from the bunch head, leaving a bubble-like channel for the bunch tail and therefore a transversely uniform wakefield, as in the nonlinear regime [10].

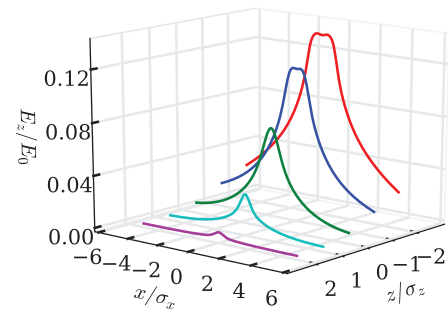

Figure 4: Distribution of E_z^b on the $x - z$ plane: $z > 0$ for the bunch head.

CONCLUSION

In this paper, the slice energy spread due to the radial dependence of the beam loading effect was analytically studied, based on the linear theory of plasma wakefield, the betatron motion and a few assumptions. In order to meet the requirement of EuPRAXIA project, the slice energy spread was optimized first by tuning the plasma density and then by increasing the laser strength. The results from 3D simulation were compared with our theory and agreed well with each other and a final slice energy spread less than 0.1% was obtained. The slice energy spread peaked near the bunch center, implying a transition from linear regime to nonlinear regime near the bunch tail when the beam density is much higher than the plasma density.

ACKNOWLEDGEMENT

This work has received funding from the European Union's Horizon 2020 research and innovation programme under grant agreement No. 653782.

REFERENCES

[1] T. Tajima and J. M. Dawson, Laser electron accelerator, Phys. Rev. Lett. 43 (1979) 267–270.

[2] E. Esarey, C. B. Schroeder and W. P. Leemans, Rev. Mod. Phys. 81 (2009) 1229–1285.

[3] Z. Huang, Y. Ding and C. B. Schroeder, Phys. Rev. Lett. 109 (2012) 204801.

[4] C. B. Schroeder, E. Esarey, C. G. R. Geddes, C. Benedetti and W. P. Leemans, Phys. Rev. ST Accel. Beams 13 (2010) 101301.

[5] P. A. Walker, *et al.*, J. Phys.: Conf. Ser. 874 (2017) 012029.

[6] X. Li, A. Mosnier and P. A. P. Nghiem, Nucl. Instrum. Methods Phys. Res. Sect. Accel. Spectrometers Detect. Assoc. Equip., (2018) 0168-9002.

[7] J.-L. Vay, *et al.*, Physics of Plasmas 18 (2011) 123103.

[8] T. Katsouleas, S. Wilks, P. Chen, J. Dawson and J. Su, Particle Accelerators 22 (1987) 81–99.

[9] W. Lu, C. Huang, M. Zhou, W. Mori and T. Katsouleas, Physics of Plasmas 12 (2005) 063101.

[10] M. Tzoufras, W. Lu, *et al.*, Physics of Plasmas 16 (2009) 056705.